Low-energy pion production in high-energy nucleus-nucleus collisions

K. Nakai and J. Chiba
Department of Physics, University of Tokyo, Tokyo, Japan
and Lawrence Berkeley Laboratory, University of California, Berkeley, California 94720

I. Tanihata and M. Sasao
Laboratory for Nuclear Studies, Osaka University, Toyonaka, Japan
and Lawrence Berkeley Laboratory, University of California, Berkeley, California 94720

H. Bowman, S. Nagamiya, and J. O. Rasmussen
Lawrence Berkeley Laboratory, University of California, Berkeley, California 94720
(Received 21 June 1979)

Doubly differential cross sections for production of pions with 400-MeV/N ^{20}Ne on C, NaF, Cu, and Pb have been measured for a range of 20 MeV $< T_\pi^{\rm LAB} <$ 100 MeV and $30° < \theta_\pi^{\rm LAB} < 150°$. The results are compared with previous data with 800-MeV/N ^{20}Ne. The broad maximum at $\theta_\pi^{\rm c.m.} = 90°$ in the center-of-mass angular distribution of low-energy pions observed at 800 MeV/N is not seen at the present energy. Neither was such a maximum at the central-rapidity region observed in (p + nucleus) reactions at $E_p = 730$ MeV. The 90° maximum seems to be a phenomenon specific to nucleus-nucleus collisions around 1 GeV/N, where the multiplicity of Δ formation is high and multiple Δ interaction could influence the pion production. The distribution at higher bombarding energies has yet to be studied.

[NUCLEAR REACTIONS C, NaF, Cu, Pb(^{20}Ne, π^+)X, E/A = 400 MeV/nucleon; measured $\sigma(E_\pi, \theta_\pi)$, E_π = 20–100 MeV, θ_π = 30°–150°.]

I. INTRODUCTION

Pion production in high-energy nucleus-nucleus collisions is of special interest because it provides unique information on the reaction mechanism. In the ($p+p$) and (p + nucleus) reactions it is well known that the mechanism of pion production in the energy range from the threshold to a few GeV is dominated by formation of the Δ(1232), so that the isobar model works well in understanding the mechanism. The formation of Δ must play an important role also in heavy-ion reactions at energies around 1 GeV/N.

We have previously measured pion production cross sections with the 800-MeV/N ^{20}Ne beam of the BEVALAC on three nuclear targets: NaF, Cu, and Pb.[2] In this work we observed that the angular distributions of pions with intermediate energies ($50 < T_\pi^{\rm c.m.} < 300$ MeV) were forward and backward peaked in the center-of-mass system, reflecting the nature of the nucleon-nucleon collision process and the formation of the Δ isobar. However, in the low-energy region ($T_\pi^{\rm c.m.} < 50$ MeV) the angular distribution was nearly isotropic, and a slight enhancement at $\theta_\pi^{\rm c.m.} = 90°$ was observed.[1,2] A broad maximum at 90° in the center-of-mass frame was barely seen and its significance was not quite convincing. However, recently a similar situation was observed in an independent measurement for 1.05-GeV/N ^{40}Ar + ^{40}Ca by Wolf *et al.*[3] This low-energy component of pion spectra seems to be specific to the nucleus-nucleus collision processes in this energy region.

We have extended the measurement of pion production cross sections to a lower beam energy, 400 MeV/N, and compared results with those at 800 MeV/N. We thought differences could arise because the energies are above and below the free nucleon threshold for formation of the Δ(1232) resonance, and indeed we observed interesting differences.

II. EXPERIMENTAL METHOD

The experimental method used to measure pion production cross sections with the 400-MeV/N ^{20}Ne was essentially the same as that used in the previous measurement at 800 MeV/N,[2] and only a brief description of the experimental method will be given here.

The 400-MeV/N ^{20}Ne beam accelerated by the BEVALAC at Lawrence Berkeley Laboratory was incident on four different targets: C, NaF, Cu, and Pb. Thicknesses of the targets were about 500 mg/cm^2 except for the C, which was 300 mg/cm^2. The NaF target was used because the average mass is approximately equal to that of the projectile ^{20}Ne, and therefore transformation of laboratory-frame cross sections to the center-of-mass frame is straightforward. The size of target was 6 cm × 6 cm. The beam intensity was measured with an ionization chamber which was calibrated against plastic scintillation counter mea-

surements of individual beam particles at lower beam intensities. The validity of extrapolating the calibration from the low beam-intensity region to higher intensity was checked in the previous experiment[2] to an accuracy of 30% by the activation method of the $^{12}C(^{20}Ne, ^{20}Ne\,n)\,^{11}C$ reaction.

A pion range telescope was used to measure low-energy positive pions from $T_\pi^{LAB}=20-100$ MeV at angles from $\theta_\pi^{LAB}=30°-150°$. The telescope was a stack of 12 plastic scintillators. For identification of pions in a strong background of protons, we used the $\pi^+ \rightarrow \mu^+$ decay. When a pion stops in one of the scintillators it generates a pair of pulses, one due to the pion and the other due to a muon emitted in the $\pi^+ \rightarrow \mu^+$ decay. Since most of negative pions are captured, making instantaneously an energetic disintegration of a carbon nucleus, only positive pions generate the double pulse. In addition to the double pulse, the ΔE vs E relation was also used by taking pulse-height information from all scintillators of the telescope. Hence, we obtained a high redundancy in identifying positive pions. A time spectrum between the π^+ and μ^+ pulses was stored for each scintillator, and the number of pions was deduced by extrapolating the time spectrum to $t=0$. The dead time in detecting the μ^+ pulse was typically 10–15 nsec. The data were taken by a PDP/11-MBD/11-CAMAC system. Details of the pion range telescope and the data-taking system are reported in a separate publication.[4]

The pion range telescope was mounted on an arm rotatable around a post on which the target was mounted.

For comparison between pion productions from high-multiplicity (more central) events and low-multiplicity (more peripheral) events, a system with eight counter telescopes, called "tag counters," was used for multiplicity tagging. The telescopes consisted of three scintillation counters, a liquid Cherenkov counter, and a copper absorber, so that crude momentum analyses and particle identification could be done. The tag-counter telescopes were mounted on a cone centered on the target with an opening angle of 40°. With this system we detected high-energy multiple particles, mainly protons with energies greater than 200 MeV emitted at $\theta^{LAB}=40°$.

III. RESULTS

Doubly differential cross sections for low-energy positive pion production with the 400-MeV/N ^{20}Ne obtained in this experiment are listed in Tables I–IV and plotted in Fig. 1. The errors shown are only statistical errors for individual numbers. The overall uncertainties for the absolute values of cross sections were about 30%.

The cross sections have been corrected for the following effects[2,4]: (a) decay in flight, (b) nuclear reactions of pions in the scintillators, (c) multiple Coulomb scattering, and (d) detector edge effect.

For comparison with the previous measurements at 800 MeV/N, contour plots of Lorentz-invariant cross sections $(1/p)(d^2\sigma/dEd\Omega)$ in a plane of $T_\pi^{c.m.}$ and $\theta_\pi^{c.m.}$ are shown in Fig. 2(a) for $(p+p)$ at 730 MeV, in 2(b) for (^{20}Ne + NaF) at 800 MeV/N, and in 2(c) for (^{20}Ne + NaF) at 400 MeV/N.

IV. DISCUSSION

A. Global behavior of pion production

In the previous measurements of pion production with the 800-MeV/N ^{20}Ne[2,5] the following results have been reported (cf. Fig. 2):

(1) The high-energy pions ($T_\pi^{c.m.} > 300$ MeV) are emitted nearly isotropically in the center-of-mass frame, and the invariant cross section has an exponential dependence on the pion energy T_π; $(1/p)(d^2\sigma/(dEd\Omega) \propto \exp(-T_\pi/T)$, with $T \sim 70$ MeV.

(2) The pions with intermediate energies ($50 < T_\pi^{c.m.} < 300$ MeV) have a forward- and backward-peaked angular distribution in the center-of-mass frame reflecting the individual nucleon-nucleon process.

(3) The low-energy pions ($T_\pi^{c.m.} < 50$ MeV) are nearly isotropic, though there seemed to exist some components which showed a slight 90° peaking in the center-of-mass angular distribution.

These results indicated that there were two groups of pions, which we shall refer to as the "direct" and the "secondary" pions.

Most of the intermediate-energy pions are direct pions, produced in formation and decay of the $\Delta(1232)$ resonance. The forward- and backward-peaked angular distribution strongly suggests this interpretation. This behavior was also observed at the present energy of 400 MeV/N. In the previous paper[2] we pointed out that gross features of pion production were generally well reproduced by the individual nucleon-nucleon collision picture: A relatively good fit of an incoherent superposition of (proton + nucleus) cross sections to the experimental (Ne + nucleus) cross section at 800 MeV/N was obtained. This result had already indicated that the direct pions were emitted not only from the peripheral collisions but also from more central collisions. In order to test this point we studied effects of the tag-counter coincidence multiplicity on the pion distributions, watching whether or not the forward/backward peak might be suppressed by the high-multiplicity (more central) tagging. No significant difference was observed between the inclusive and the tagged distributions.

There must also be pions emitted after some statistical processes in nuclei such as scattering,

TABLE I. Cross section for π^+ from 400-MeV/N ^{20}Ne on the C in μb/sr MeV. The numbers in parentheses are statistical uncertainties. The overall uncertainty is 30%.

Pion energy (MeV)	Angle (deg.) 30	45	60	75	90	105	120	150
19	14.8 (2.0)	15.9 (1.5)	19.9 (1.6)	22.5 (1.3)	24.9 (1.1)	20.9 (1.0)	21.4 (1.2)	22.2 (1.2)
29	23.1 (2.4)	22.3 (1.9)	22.5 (2.2)	27.5 (1.3)	28.1 (1.1)	27.1 (1.0)	25.9 (1.3)	23.3 (1.3)
40	22.0 (4.5)	25.2 (2.7)	29.0 (2.5)	33.7 (1.5)	33.2 (1.1)	31.0 (1.1)	27.8 (1.4)	26.2 (1.4)
49	35.5 (3.6)	36.1 (1.8)	35.8 (1.9)	35.8 (1.2)	34.6 (1.0)	30.3 (1.0)	27.7 (1.3)	21.2 (1.1)
61	46.1 (3.2)	39.5 (1.9)	33.7 (1.9)	37.6 (1.6)	30.9 (1.0)	27.0 (1.0)	20.9 (0.9)	17.6 (1.0)
76	45.2 (4.8)	40.6 (2.8)	36.0 (2.5)	29.7 (1.7)	24.9 (1.1)	19.1 (1.0)	17.0 (1.2)	8.8 (0.9)
86	49.0 (5.5)	45.5 (3.8)	34.3 (3.2)	27.1 (1.7)	22.7 (1.4)	15.2 (1.0)	12.0 (1.0)	4.6 (0.6)
93	51.0 (6.8)	41.9 (3.4)	32.5 (3.4)	25.5 (1.4)	20.6 (1.2)	12.1 (1.3)	10.2 (0.9)	4.8 (0.6)
102	50.4 (5.9)	38.8 (2.3)	27.4 (2.3)	20.3 (1.1)	14.6 (0.9)	10.0 (0.6)	6.9 (0.5)	3.0 (0.5)

TABLE II. Cross section for π^+ from 400-MeV/N ^{20}Ne on the NaF in μb/sr MeV. The numbers in parentheses are statistical uncertainties. The overall uncertainty is 30%.

Pion energy (MeV)	Angle (deg.) 30	45	60	75	90	105	120	150
19	23.3 (2.4)	23.8 (2.1)	32.0 (1.5)	34.3 (1.3)	38.0 (1.4)	31.1 (2.2)	35.3 (1.3)	35.6 (2.0)
29	35.5 (3.1)	35.3 (3.2)	39.7 (2.1)	42.5 (1.8)	46.2 (1.6)	45.9 (2.3)	44.2 (1.5)	37.0 (2.0)
40	44.7 (7.1)	42.1 (4.5)	51.8 (2.1)	53.0 (2.0)	52.5 (1.8)	51.7 (2.4)	46.4 (1.5)	44.2 (2.1)
49	48.2 (4.3)	55.7 (4.2)	57.1 (1.9)	56.6 (1.5)	54.4 (1.5)	55.2 (2.3)	45.2 (1.4)	34.9 (1.6)
61	71.6 (4.9)	61.6 (4.0)	54.8 (1.8)	56.6 (1.5)	52.4 (1.6)	43.6 (1.8)	37.3 (1.0)	26.8 (1.2)
76	70.9 (6.1)	63.7 (4.9)	51.5 (2.4)	48.7 (2.3)	37.6 (1.8)	27.1 (2.0)	23.9 (1.5)	17.7 (1.4)
86	80.4 (8.1)	60.5 (6.5)	52.9 (3.3)	43.1 (2.9)	32.9 (1.8)	16.9 (2.5)	17.8 (1.5)	11.4 (1.3)
93	81.4 (9.4)	60.6 (6.5)	51.4 (2.8)	38.5 (2.0)	31.6 (1.8)	17.6 (2.4)	15.2 (1.2)	8.4 (1.2)
102	83.6 (6.0)	59.5 (5.4)	40.7 (1.7)	29.8 (1.5)	21.6 (1.0)	15.0 (1.5)	9.6 (0.7)	6.4 (0.8)

TABLE III. Cross section for π^+ from 400-MeV/N ^{20}Ne on the Cu in μb/sr MeV. The numbers in parentheses are statistical uncertainties. The overall uncertainty is 30%.

Pion energy (MeV)	Angle (deg.) 30	45	60	75	90	105	120	150
19	42.9 (5.5)	42.2 (6.0)	53.9 (3.8)	56.3 (3.2)	68.1 (4.5)	54.2 (4.0)	67.9 (3.6)	77.6 (3.2)
29	67.3 (9.2)	70 (10)	76.0 (3.7)	80.5 (3.6)	89.4 (3.8)	88.1 (3.5)	91.5 (3.3)	90.2 (4.7)
40	102 (20)	73 (13)	93.2 (5.6)	97.5 (4.0)	112 (5)	92.2 (3.3)	106 (4)	96.5 (4.6)
49	105 (10)	94 (10)	108 (4)	102 (4)	118 (4)	98.8 (3.3)	91.4 (3.6)	88.8 (3.6)
61	121 (11)	110 (10)	102 (5)	110 (4)	103 (4)	84.8 (2.9)	78.7 (2.5)	65.5 (3.2)
76	125 (15)	100 (14)	94.0 (5.5)	78.8 (4.2)	85.1 (3.9)	56.7 (4.0)	54.2 (3.4)	38.5 (3.2)
86	134 (22)	89 (18)	92.5 (6.1)	73.2 (4.9)	60.3 (4.6)	42.4 (4.0)	35.4 (2.7)	30.3 (3.3)
93	140 (16)	87 (16)	86.2 (8.1)	73.3 (4.3)	56.3 (5.8)	45.6 (3.6)	35.1 (1.2)	32.4 (2.8)
102	145 (13)	85 (13)	70.7 (4.4)	62.0 (3.7)	46.9 (3.4)	29.0 (2.5)	24.9 (1.7)	15.4 (1.8)

TABLE IV. Cross section for π^+ from 400-MeV/N ^{20}Ne on the Pb in μb/sr MeV. The numbers in parentheses are statistical uncertainties. The overall uncertainty is 30%.

Pion energy (MeV)	Angle (deg.) 30	45	60	75	90	105	120	150
19	55 (11)	45 (10)	32 (10)	48 (8)	77 (8)	51 (9)	60 (10)	101 (10)
29	88 (21)	89 (16)	66 (9)	80 (7)	105 (7)	121 (7)	125 (8)	153 (10)
40	171 (38)	134 (21)	87 (12)	129 (7)	141 (10)	137 (7)	145 (10)	183 (13)
49	168 (24)	141 (17)	122 (9)	125 (7)	146 (7)	140 (7)	141 (8)	163 (9)
61	186 (25)	155 (17)	110 (9)	137 (7)	142 (6)	133 (5)	115 (6)	123 (8)
76	163 (37)	142 (20)	102 (11)	102 (9)	113 (7)	100 (8)	93.5 (6.6)	71.8 (8.3)
86	179 (42)	158 (24)	101 (13)	103 (10)	82 (10)	85.2 (7.5)	63.5 (8.1)	38.1 (8.6)
93	208 (43)	159 (23)	98 (10)	98.4 (8.2)	85.8 (9.3)	70.0 (6.7)	56.9 (6.7)	39.6 (6.7)
102	230 (32)	158 (18)	81.5 (7.2)	69.3 (5.9)	66.3 (5.0)	52.1 (4.2)	42.2 (4.3)	19.4 (4.2)

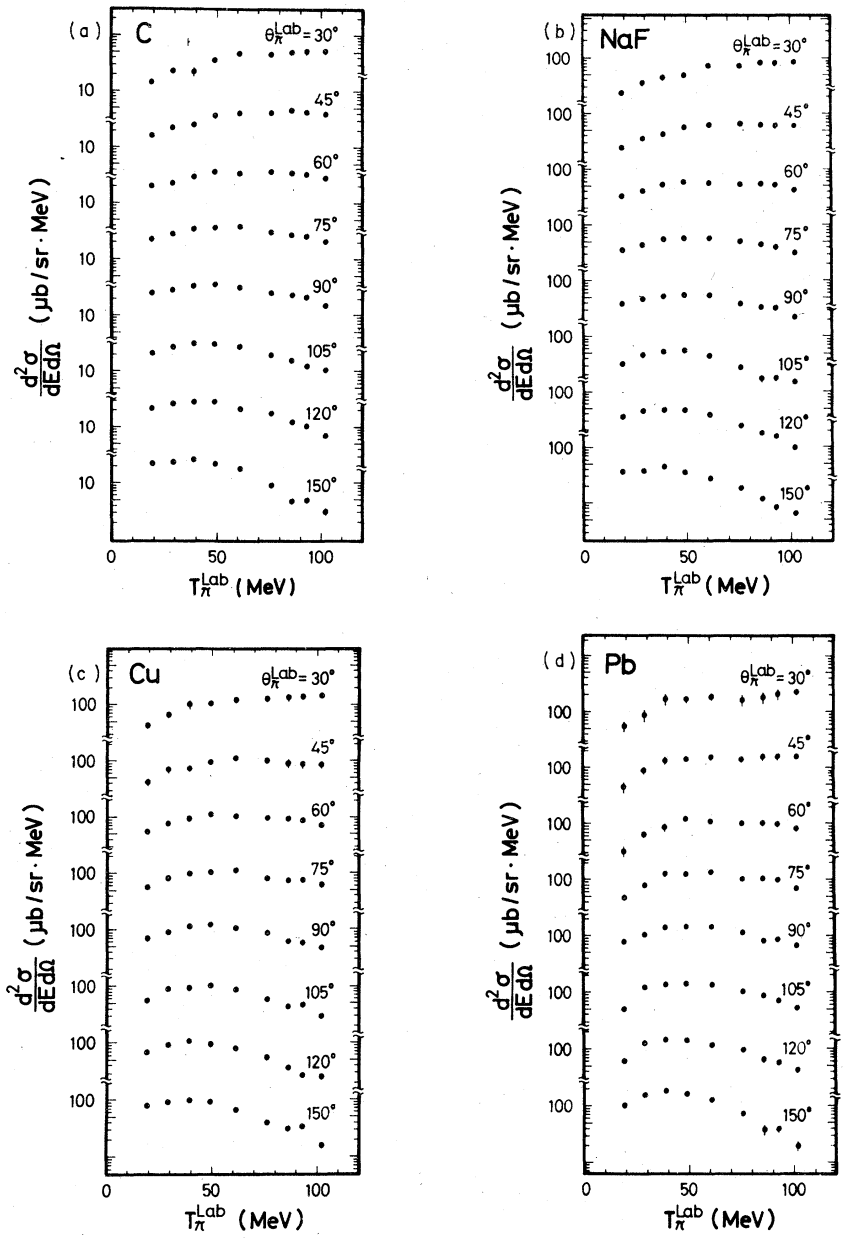

FIG. 1. Doubly differential cross sections for positive pion productions with 400-MeV/N ^{20}Ne on (a) C, (b) NaF, (c) Cu, and (d) Pb targets.

charge exchange, absorption, and reemission. The statistical nature of the processes would produce an exponential-type energy dependence (of the invariant cross section) with a parameter T. When the statistical processes are well developed to reach at an equilibrium state, the parameter T represents the temperature of the pionic ensemble. The system may be partially thermalized and those pions may be called "thermalized" pions, but we chose not to do so and called them more generally "secondary" pions. The exponential energy dependence was seen in the high-energy region. Although it was not seen at the intermediate-energy region because the direct pions dominated, there must be components of the secondary pions in this region too.

Shown in Fig. 3 are pion momentum spectra at 90° and 150° in the center-of-mass frame. Experimental data of three measurements, from Refs. 2 and 5, and the present one, are sum-

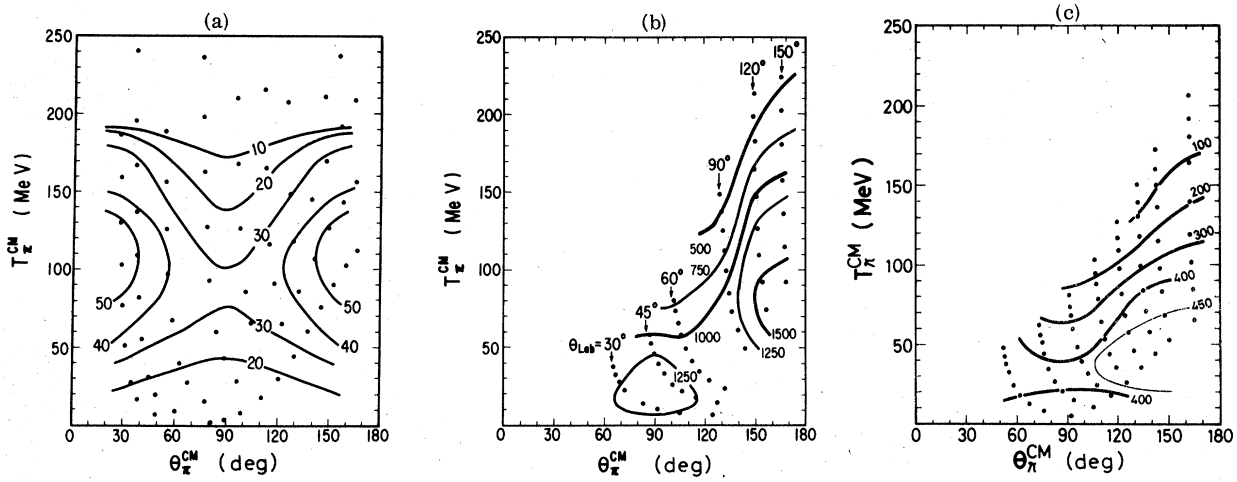

FIG. 2. Contour plots of the Lorentz-invariant cross sections for (a) $p+p\rightarrow\pi^+ +\chi$ at 730 MeV, (b) ^{20}Ne+NaF$\rightarrow\pi^+ +\chi$ at 800 MeV/N, and (c) ^{20}Ne+NaF$\rightarrow\pi^+ +\chi$. The numbers written along contour lines are Lorentz-invariant cross sections in units of mb sr^{-1} (GeV)$^{-2}$ c. The dots in the figure indicate observed points. The contour lines should be symmetric about $\theta_\pi^{c.m.}=90°$.

marized. We can estimate the secondary-pion component by extrapolating the $\exp(-T_\pi/T)$ spectrum from the high-energy region.[5] Then, the figure shows that the pions at 90° are mainly secondary pions, while at $\theta_\pi^{c.m.}=150°$ both direct and secondary pions contribute to the energy spectrum.

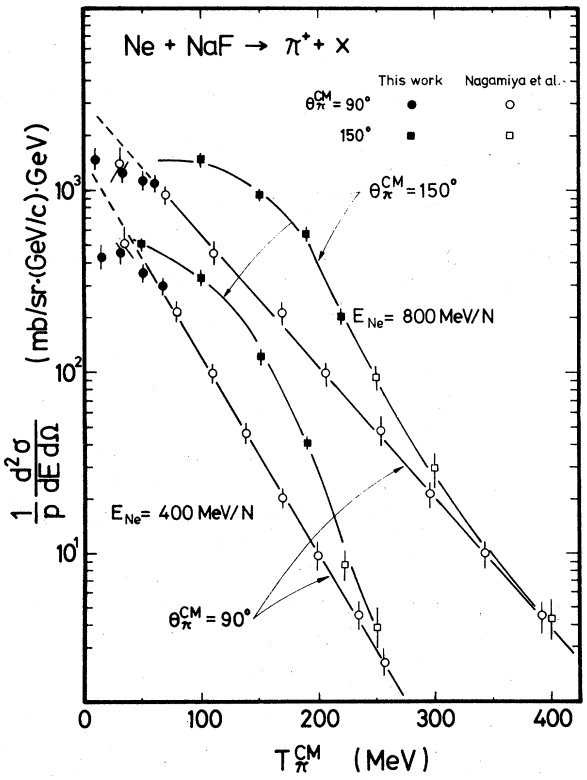

FIG. 3. Pion momentum distributions at $\theta_\pi^{c.m.}=90°$ and 150°. Experimental data from Refs. 2 and 4 were used.

The bending at the low-energy end is due to the Coulomb effect.

B. On the broad maximum at $\theta_\pi^{c.m.}=90°$

We noted in the data with 800-MeV/N ^{20}Ne that though the angular distribution of low-energy pions was nearly isotropic, there existed some pions which were emitted preferentially to 90° in the center-of-mass frame.[1,2] Being stimulated by this observation, we started the present experiment at 400 MeV/N. We thought that the bump might be an indication of the hydrodynamic flow of nuclear

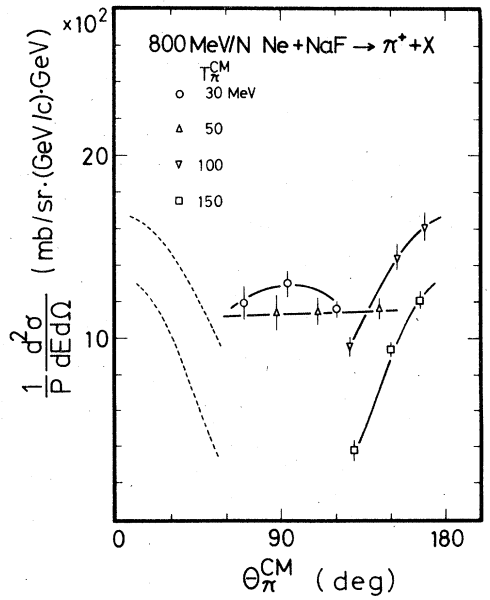

FIG. 4. Center-of-mass angular distributions of pions with different center-of-mass energies.

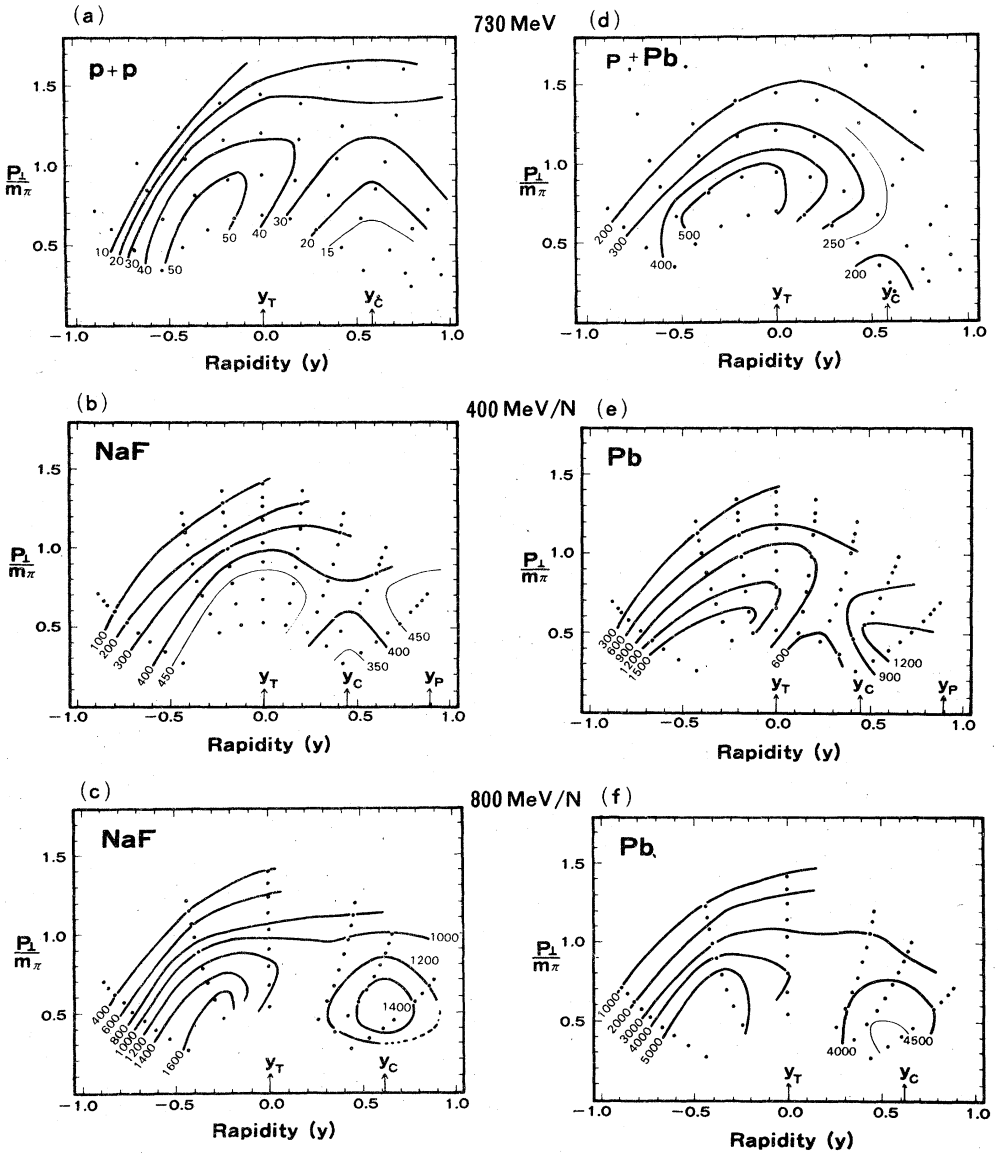

FIG. 5. Contour plots of Lorentz-invariant cross sections in $p_\perp$ (transverse momentum) and y (rapidity) plane for (a) $p+p$ at 730 MeV, (b) ^{20}Ne+NaF at 400 MeV/N, (c) ^{20}Ne+NaF at 800 MeV/N, (d) $p+$Pb at 730 MeV, (e) ^{20}Ne+Pb at 400 MeV/N, (f) ^{20}Ne+Pb at 800 MeV/N. The numbers written along contour lines are the Lorentz-invariant cross sections in units of mb sr^{-1} GeV^{-2} c. The dots indicate observed points.

matter and, if so, the same or even more enhanced bump should be seen at the lower collision energy. However, we observed no bump at 400 MeV/N and found a significant difference in the low-energy pion distributions.

Results of the previous experiments are shown in Fig. 2. Figure 2(b) is a contour plot of the invariant cross section in the center-of-mass angle and kinetic-energy plane for the (^{20}Ne + NaF $\rightarrow \pi^+ + x$) process at 800 MeV/N. For comparison, the same plot for the ($p + p \rightarrow \pi^+ + x$) process at 730 MeV is shown in Fig. 2(a). Cuts of the contour plot at several different pion c.m. energies are shown in Fig. 4. In contrast to the pions with energies higher than 100 MeV, which show forward and backward peaking in the angular distributions, the low-energy pions ($T_\pi^{\text{c.m.}} < 30$ MeV) are emitted with an angular distribution enhanced at $\theta_\pi^{\text{c.m.}} = 90°$. If we subtract the contribution of the nucleon-nucleon process from the pion distribution from the (^{20}Ne + NaF) reaction, the 90° peak would be more enhanced.

The contour plot of the 400-MeV/N data is shown in Fig. 2(c). The angular distribution of intermediate-energy pions is forward and backward peaked. The maximum around $\theta_\pi^{\text{c.m.}} = 90°$ is not

TABLE V. Appearance of the broad maximum at the "central" region of pion distribution.

MeV/N	$A+A$	$p+A$	$p+p$
~800	Yes	No	No
~400	No	...	...

seen, though the bumps at the intermediate-energy region are similar to the 800-MeV/N data.

In order to extend the comparison to heavier targets and also to (p + nucleus) processes, where the center-of-mass frame is not uniquely defined, we plotted the invariant cross section $(1/p)(d^2\sigma/dEd\Omega)$ in the rapidity ($y=\frac{1}{2}\ln[(E+P_{\parallel})/(E-P_{\parallel})]$) and transverse momentum ($p_{\perp}$) plane. Then, the shape of distribution is independent of the Lorentz frame.

Shown in Fig. 5 are plots for (a) $p+p$ at 730 MeV, (b) ^{20}Ne + NaF at 400 MeV/N, (c) ^{20}Ne + NaF at 800 MeV/N, (d) p + Pb at 730 MeV, (e) ^{20}Ne + Pb at 400 MeV/N, and (f) ^{20}Ne + Pb at 800 MeV/N. The arrows in the figures indicate the rapidities of target (y_T) and projectile (y_P) and the central rapidity [$y_C=\frac{1}{2}(y_P+y_T)$]. The bump around $\theta_\pi^{\text{c.m.}}=90°$ and $T_\pi^{\text{c.m.}}=30$ MeV in Fig. 2(b) can now be seen as the bump at the central region around $y_C=0.61$ in Fig. 5(c). The bump in the central region is also seen in the (^{20}Ne + Pb) process at 800 MeV/N [Fig. 5(f)]. We note, however, that the bump does not appear in the 400-MeV/N data [Figs. 5(b) and 5(e)], nor in the (proton + nucleus) data [Fig. 5(d)]. We may summarize the situation as shown in Table V.

It is, of course, difficult to deny the existence of such a small effect in the 400 MeV/N data from the present experiment. However, similar results have also been reported by Wolf *et al.*[3] in their measurements of the (^{40}Ar + ^{40}Ca) collisions at 1.05 GeV/N and 400 MeV/N.

The fact that the 90° bump (or the "central" bump) appears only at the higher bombarding energy limits possibilities of our explaining the mechanism which results in the bump. The effects such as (1) hydrodynamic splashing,[6] (2) shadowing, and (3) Coulomb effect could partly be in the mechanism of forming the bump, but do not explain the difference.

As discussed in the Introduction, the difference between the 800-MeV/N reaction and the 400-MeV/N reaction is in the mean multiplicity of formation of the Δ. The effective free nucleon-nucleon threshold for the Δ formation is between the two energies. Although the Δ resonance can be formed at 400 MeV/N by the aid of Fermi motion, the multiplicity must be much less than that at

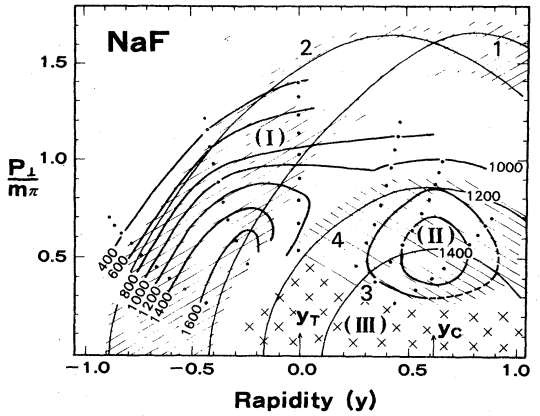

FIG. 6. Kinematic domains of pions from decay of a single Δ (region I) and those from other origins, possibly from multiple-Δ states (region II). The curves 1 and 2 correspond to pions from a Δ moving forward and backward, respectively, in a nucleon-nucleon collision. The curves 3 and 4 correspond to pions emitted in the central region with energies of 20 and 50 MeV. The contour lines of experimental cross sections are from Fig. 5(c). The Coulomb effect suppresses the positive-pion yields in the region shown by crosses (region III).

800 MeV/N. Vary pointed out that the multiplicity of pion production is roughly proportional to the pion production cross section in the nucleon-nucleon process.[7] We can extend this argument to the Δ-formation multiplicity because at this energy region the pion production is mainly through the formation of the Δ isobar. Then the multiplicity of Δ formation at 800 MeV/N can be estimated to be 10 times as large as that at 400 MeV/N.

The difference between the data with 800-MeV/N ^{20}Ne and 730-MeV proton could also be ascribed to the multiplicity difference of Δ formation. The multiplicity of Δ by the ^{20}Ne reactions could be at least 10 times more than that of proton reactions.

These considerations led us to attribute the low-energy central bump observed only with 800-MeV/N ^{20}Ne to multiple-Δ formation. However, such low-energy pions are not available from a decay of single Δ. In Fig. 6 the possible kinematic domain for a pion emitted from a single Δ is shown (region I, hatched zone). The curves 1 and 2 correspond to pions from the Δ moving forward and backward, respectively, in the nucleon-nucleon collision. The pions emitted in the decay of the Δ are distributed around these curves because of angular and mass distributions of the Δ. The domain does not cover the central bump. The pions from a single Δ have too much energy to explain the bump.

The Coulomb effect is another important factor for the low-energy pion distribution. As shown

experimentally by Benenson *et al.*[8] the effect suppresses the pion yields in the region near ($y \simeq y_P$, $p_\perp \simeq 0$) and ($y \simeq y_T$, $p_\perp \simeq 0$). If we believe the existence of "Fireball," or the central part, the suppression would occur also around ($y = y_C$, $p_\perp \simeq 0$). In Fig. 6, those regions are indicated by crosses (region III). This effect seems to be an important factor in forming the central bump. However, the difference between the data at 800 MeV/N and 400 MeV/N is not explainable by the Coulomb effect alone.

Recently, the existence of deeply bound Δ–Δ (dibaryon) states has been shown theoretically[9] and experimentally.[10] If such multiple-Δ bound states were formed, the energies of pions from their decay should be lower than those from the single-Δ decay. The curves 3 and 4 in Fig. 6 correspond to pions emitted with energies of 20 and 50 MeV from a state with the central rapidity $y_C = \frac{1}{2}(y_P + y_T)$. It seems to be necessary to consider such a mechanism to explain the low-energy central bump (region II).

The available experimental information is not sufficient to check the argument further, and we are not able to stress it strongly. It should be emphasized, however, that those low-energy central bumps, which were observed in the collisions of 800-MeV/N ^{20}Ne but not of 730-MeV protons with nuclei, must have an interesting origin specific to the high-energy nucleus-nucleus collisions.

At 800 MeV the cross section for formation of Δ in a p–p collision (~20 mb) is as large as a half of the p–p total cross section(~40 mb), so that when nuclei collide at 800 MeV/N a quarter of the participating nucleons become Δ. Such a situation can be produced only by nucleus-nucleus collisions in this energy region. It is of great interest to study the pion production more systematically and by observing correlations.

ACKNOWLEDGMENTS

The possibility of forming the multiple-Δ matter in heavy-ion reactions had been pointed out by the late Professor J.-I. Fujita, long before we started these experiments.[11] We were encouraged by his stimulating discussions and continuous interest. We are grateful to the BEVALAC staff and operators for their support of the experiments. We wish to thank Professor Sugimoto and Professor Fukui for their advice and support for the experiment. We thank Dr. J. Ingersoll, Dr. R. S. Hayano, and Miss M. Sekimoto for their help at various stages of the experiment. This work was supported by the Mitsubishi Foundation (Japan), by the Nuclear Physics Division of the U.S. Department of Energy, and by the Japan Society for Promotion of Science, and had the endorsement of the National Science Foundation. One of us (J.O.R.) wishes to acknowledge the travel support of the National Science Foundation for a trip to Japan to work with Japanese colleagues on completion of this paper, and to work on other collaborative research.

[1]K. Nakai, J. Chiba, I. Tanihata, S. Nagamiya, H. Bowman, J. Ioannou, and J. O. Rasmussen, contribution to the VIIth International Conference on High-Energy Physics and Nuclear Structure, Zürich, August, 1977 (unpublished).

[2]J. Chiba, K. Nakai, I. Tanihata, S. Nagamiya, H. Bowman, J. Ingersoll, and J. O. Rasmussen, Phys. Rev. C 20, 1332 (1979).

[3]K. L. Wolf, H.H. Gotbrod, W. G. Meyer, A. M. Poskanzer, A. Sandoval, R. Stock, J. Gosset, C. H. King, G. King, Nguyen Van Sen, and G. D. Westfall, Phys. Rev. Lett. 22, 1448 (1979).

[4]J. Chiba, thesis, 1979, Report No. UTPN-130 (unpublished).

[5]S. Nagamiya, I. Tanihata, S. Schnetzer, L. Anderson, W. Bruckner, O. Chamberlain, G. Shapiro, and H. Steiner, in Proceedings of the International Conference on Nuclear Structure, Tokyo, 1977 [J. Phys. Soc. Jpn. 44, Suppl. 378 (1978)].

[6]W. Scheid, H. Muller, and W. Greiner, Phys. Rev. Lett. 32, 741 (1974); Y. Kitazoe and M. Sano, Lett. Nuovo Cimento 14, 407 (1975).

[7]J. Vary, Phys. Rev. Lett. 40, 295 (1978).

[8]W. Benenson *et al.* (private communication).

[9]T. Kamae and T. Fujita, Phys. Rev. Lett. 38, 471 (1977).

[10]T. Kamae, I. Arai, T. Fujii, H. Ikeda, N. Kajiura, S. Kawabata, K. Nakamura, I. Ogawa, T. Takada, and Y. Watase, Phys. Rev. Lett. 38, 468 (1977).

[11]J.-I. Fujita, Butsuri 30, 344 (1975).